Eur. Phys. J. Plus (2026) 141:740
https://doi.org/10.1140/epjp/s13360-026-07931-y

THE EUROPEAN PHYSICAL JOURNAL PLUS

Regular Article

Investigating the production of ^{99m}Tc via the ^{98}Mo(n, γ)^{99}Mo reaction at a high-current accelerator-based neutron source

Doruntin Shabani[1,2,3,a], **Christoph Langer**[1], **Eric Mauerhofer**[3], **Paul Zakalek**[3], **Jingjing Li**[3], **Thomas Gutberlet**[3]

[1] FH Aachen University of Applied Sciences, Campus Jülich, 52428 Jülich, Germany
[2] Institute for Nuclear Physics, University of Cologne, 50937 Cologne, Germany
[3] Jülich Centre for Neutron Science, Forschungszentrum Jülich GmbH, 52425 Jülich, Germany

Received: 6 March 2026 / Accepted: 4 June 2026

Abstract Ensuring a reliable and uninterrupted supply of the essential medical isotope, technetium-99m (^{99m}Tc), remains a major technical and organizational challenge. Because of its short half-life, ^{99m}Tc is commonly obtained from ^{99}Mo/^{99m}Tc generators, making a continuous supply of molybdenum-99 (^{99}Mo) crucial for nuclear medicine. The production of ^{99}Mo via the ^{98}Mo(n,γ)^{99}Mo reaction was investigated by Monte Carlo simulations with PHITS for a High-Current Accelerator-based Neutron Source (HiCANS) modeled after the High Brilliance neutron Source (HBS) design. Target-moderator-reflector (TMR) configurations were systematically varied to optimize neutron capture in natural Mo, with an H_2O moderator and MgO reflector identified as the most practical setup. A 3-cm-thick Mo plate provided the best balance between total yield and specific activity suitable for low specific activity (LSA) ^{99}Mo/^{99m}Tc generators, while concentrating irradiation on a proton beam-aligned plate appears advantageous for both yield and handling. The results suggest that HiCANS facilities such as the HBS could supply regional ^{99}Mo demand without relying on fission reactors, while reducing waste and proliferation concerns.

1 Introduction

Technetium-99m (^{99m}Tc), derived from its precursor molybdenum-99 (^{99}Mo), is used in 80% of nuclear medicine diagnostic procedures (~30 million annually), with ~25% of demand in Europe and Germany alone performing ~60,000 procedures weekly [1, 2]. The short half-lives of ^{99}Mo (66 h) and ^{99m}Tc (6 h) pose significant challenges. Disruptions in the production chain can delay or cancel important medical procedures, with consequent effects on patients, their treatment, and their health [3].

^{99}Mo is generally produced by fission of uranium-235 (^{235}U) by irradiating enriched ^{235}U targets in nuclear reactors [4, 5]. This ^{99}Mo production pathway is very effective due to the high fission cross section of ^{235}U (585 b) for thermal neutrons and the high cumulative fission yield of ^{99}Mo (6.1%). About 26,000 Ci per week of ^{99}Mo are shipped weekly from about 11 reactors worldwide [1]. However, this production route generates significant radioactive waste and necessitates complex radiochemical processing and non-proliferation measures. In Germany alone, the clinical demand corresponds to roughly 2,400 Ci (activity at the end of irradiation) of ^{99}Mo per week, underlining the importance of reliable alternative production methods [1].

Neutron capture of natural Mo via ^{98}Mo$(n,\gamma)^{99}$Mo is the most direct non-^{235}U-fission approach, where ^{98}Mo has an isotopic abundance of 24.29% [6–10]. To achieve meaningful ^{99}Mo activity through neutron capture, a high epithermal flux is required due to the significantly higher radiative capture integral of ^{99}Mo (6.5 barns) compared to its thermal cross section (0.13 barns) [11]. Though producing low specific activity (LSA) ^{99}Mo, compared to fission of ^{235}U, this method offers the advantages of a simplified processing scheme and significantly reduced radioactive waste generation.

Several other alternative production routes were explored, including proton bombardment and fast neutron capture, photo-neutron, and photo-fission processes [12–17]. In the proton-induced method, ^{99m}Tc is produced directly via the ^{100}Mo(p,2n)^{99m}Tc reaction using enriched ^{100}Mo targets, but its short half-life limits distribution to regional use. Photo-neutron production relies on bremsstrahlung photons from an electron accelerator to induce the (γ,n) reaction in ^{100}Mo, while photo-fission involves photon-induced fission of uranium targets; both methods face technical challenges such as high thermal power densities in the targets and relatively lower production efficiencies [17].

Table 1 summarizes representative accelerator-based production routes for ^{99}Mo, highlighting differences in reaction mechanisms, target materials, and production yields.

[a] e-mail: shabani@fh-aachen.de (corresponding author)

Published online: 24 June 2026

Table 1 Comparison of accelerator-based ^{99}Mo production routes based on EOI-equivalent activity [18, 19]

Facility/study	Production pathway	Beam type and energy	Target material	Reported output
NorthStar medical radioisotopes	^{100}Mo(γ, n)^{99}Mo	Electrons 40 MeV	Enriched ^{100}Mo	2300 Ci/week per target station
TRIUMF	^{100}Mo(p, 2n)^{99m}Tc	Protons 16–24 MeV	Enriched ^{100}Mo	300–800 Ci/week ^{99m}Tc
SHINE Technologies	^{235}U(n, fission)^{99}Mo	D-T ~ 14 MeV neutrons	LEU < 20% ^{235}U	~ 15,000 Ci/week

As shown in Table 1, accelerator-based ^{99}Mo production routes differ significantly in reaction mechanism, target requirements, and achievable activity. Fission-based systems (e.g., SHINE Technologies) provide the highest production levels and high specific activity (HSA) ^{99}Mo. Photonuclear approaches (e.g., NorthStar) yield lower activities and require enriched ^{100}Mo, producing LSA ^{99}Mo. Cyclotron-based methods (e.g., TRIUMF) generate ^{99m}Tc directly and do not follow the generator supply model.

As large research reactors that currently supply most of the global ^{99}Mo inventory face periodic maintenance and age-related shutdowns, it is important to assess whether these accelerator-based neutron sources could help stabilize the supply. The High Brilliance neutron Source (HBS) is a proposed high-current accelerator-based neutron source (HiCANS) concept at Forschungszentrum Jülich in which fast neutrons are produced by protons impinging on a tantalum (Ta) target in a compact target-moderator-reflector (TMR) assembly. Under the HBS design parameters considered here, a 70 MeV proton beam with an average current of 12 mA (12% duty cycle) impinges on a water-cooled Ta target designed for heat fluxes up to 3 kW/cm^2 [20]. While the HBS is primarily designed for neutron-scattering research, we assess the feasibility of using HBS-type TMR for regional ^{99}Mo production via ^{98}Mo(n,γ)^{99}Mo. The objective of this study is the end-of-irradiation ^{99}Mo activity achievable for a 6-day irradiation, subject to maintaining a specific activity compatible with LSA ^{99}Mo/^{99m}Tc generator concepts and the selection of moderator/reflector solutions that remain practical from an engineering perspective. Neutron spectra and fluxes in natural Mo plates are obtained from Monte Carlo simulations with the Particle and Heavy Ion Transport code System (PHITS), which was previously benchmarked against neutron activation experiments to validate its ability to reproduce activation in neutron fields [21]. These simulations are then used to quantify attainable ^{99}Mo yields and specific activities for systematically varied TMR configurations and to assess the contribution of such a facility to Germany's weekly ^{99}Mo demand.

2 Methodology

The activity A (Bq) of ^{99}Mo produced via the ^{98}Mo(n,γ)^{99}Mo reaction during irradiation of a Mo sample of natural isotopic abundance was calculated according to [21]:

$$A = \frac{m}{M}\mathrm{Nh}\left(\sigma_{th}\phi_{th} + I_{\gamma}(\alpha)\phi_{epi} + \sigma_{fast}\phi_{fast}\right)\left(1 - e^{-\frac{\ln(2)\,t_b}{t_{1/2}}}\right) \quad (1)$$

where m (g) is the sample mass, N is the Avogadro number, M is the molar mass (M = 95.94 g/mol), h is the abundance of ^{98}Mo (h = 0.2419), t_b is the irradiation time (t_b = 144 h), $t_{1/2}$ is the half-life of ^{99}Mo ($t_{1/2}$ = 65.94 h). The microscopic cross sections include the thermal neutron cross section (σ_{th} = 0.131 b [22]), the resonance integral $I_\gamma(\alpha)$, which depends on the neutron spectrum shape parameter α (with $I_\gamma(0)$ = 6.552 b [22]), and the effective fast neutron cross section σ_{fast} obtained by convoluting the energy-dependent cross section from the JENDL-4.0 library with the simulated fast neutron spectrum. ϕ_{th}, ϕ_{epi}, ϕ_{fast} represent the thermal, epithermal, and fast neutron fluxes within the sample, respectively. These fluxes were obtained from PHITS simulations and converted from per-primary quantities to physical units of cm^{-2}s^{-1} by normalization to the assumed proton beam current. The neutron spectrum shape parameter α and the corresponding resonance integral $I_\gamma(\alpha)$ were determined from the simulated neutron spectra following the procedure described in [21]. Additional estimates were performed to evaluate the contribution of ^{100}Mo(n,2n)^{99}Mo reaction channel. The corresponding increase in predicted activity remained within approximately 13% of the reported values. In this work t_b, h, M, $t_{1/2}$, σ_{th}, and $I_\gamma(0)$ were treated as fixed inputs, while TMR configuration and plate position were varied in the parameter scans. The quantities ϕ_{th}, ϕ_{epi}, ϕ_{fast}, and α (and therefore $I_\gamma(\alpha)$ and σ_{fast}) were obtained from the simulation output files for each individual configuration. The mass m was determined by the modeled Mo plate geometry and varies only with plate thickness. The predicted activities are subject to uncertainties associated with Monte Carlo statistical errors, nuclear data evaluations, and geometrical modeling assumptions. PHITS [23] was previously benchmarked against neutron activation experiments using an Americium-Beryllium (AmBe) neutron source and demonstrated agreement between simulations and experimental measurements within approximately 15% [21]. In addition, variations between evaluated nuclear data libraries may contribute to the overall predictive uncertainty. Although a dedicated sensitivity analysis using multiple nuclear data libraries was beyond the scope of the present parameter study, previous experience with comparable activation calculations indicates that the effects remain limited and would not alter the main conclusions of the present work.

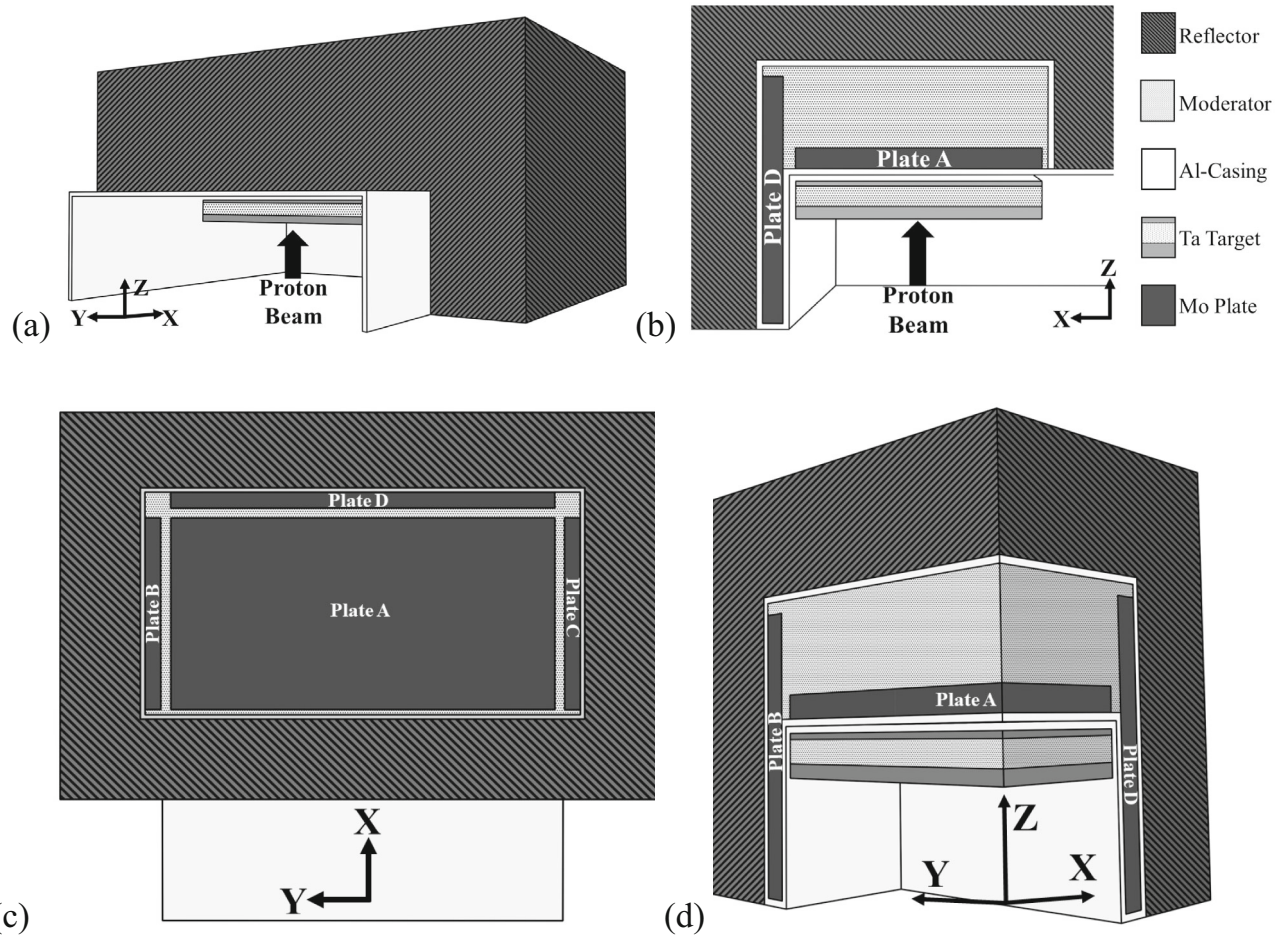

Fig. 1 Conceptual design of the TMR assembly and the arrangement of the Mo plates: **a** full 3d model, **b** cut along the xz-plane, **c** cut along the xy-plane, and **d** cut at the x–y origin

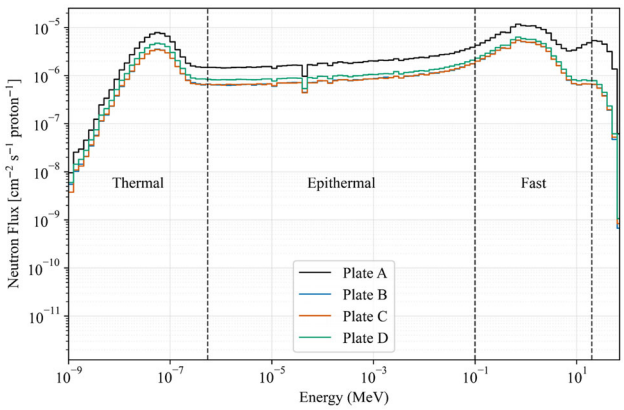

Fig. 2 Neutron energy spectra for the plates positioned at 2 cm distance from the Al casing with 5-cm H_2O moderator and Pb reflector thickness

3 Simulations

The fast, epithermal, and thermal fluxes within the Mo plates were extracted using Monte Carlo particle transport simulations PHITS v3.22 with the JENDL-4.0 nuclear data library [24]. Each simulation was performed with 10^8 primary source particles. A homogenous 70 MeV proton beam impinges on a Ta target producing fast neutrons, which are then moderated and reflected by surrounding materials.

Moderator materials were selected based on high slowing-down power, favorable moderating ratio, and low-neutron absorption cross sections [25, 26]. Four candidates were investigated: light water (H_2O), heavy water (D_2O), beryllium (Be), zirconium hydride (ZrH_2). Reflector materials were chosen for low absorption and high scattering cross sections [26], with three candidates evaluated:

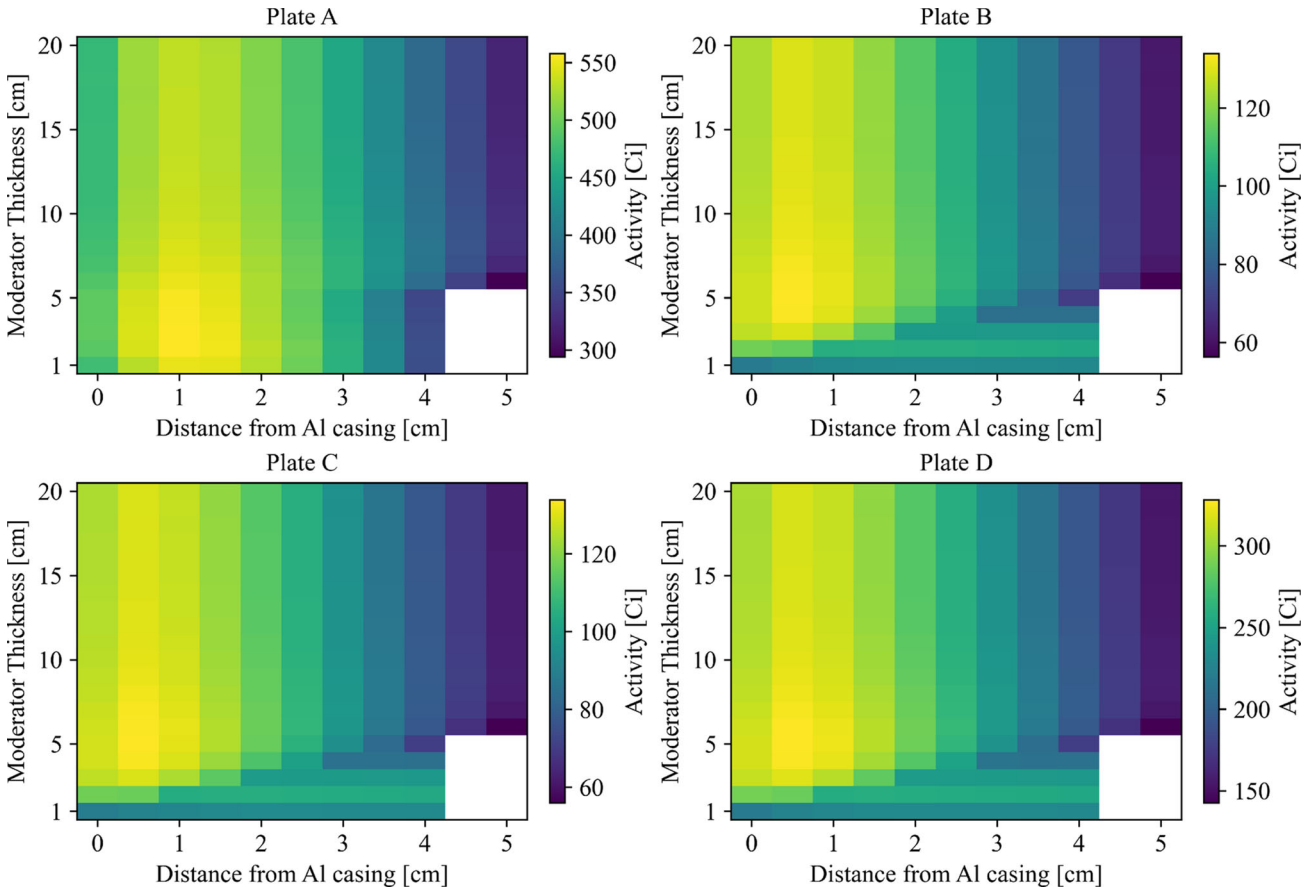

Fig. 3 ^{99}Mo activity (Ci) for an H_2O moderator and Pb reflector (5 cm thickness)

lead (Pb), magnesium oxide (MgO), and beryllium (Be). Elemental compositions and mass densities for all materials in the PHITS model were taken from [27].

The geometry of the simulated TMR assembly is shown in Fig. 1. The Ta target has a surface area of 12×24 cm^2 and consists of a 0.6-cm Ta layer, a 1-cm water layer acting as the proton beamstop, and a 0.25-cm Ta back layer, leading to a total thickness of 1.85 cm. This configuration produces fast neutrons and can handle heat fluxes up to 3 kW/cm^2 under active cooling [28, 29]. In this TMR design, a 0.3-cm-thick aluminum (Al) casing is placed 0.3-cm downstream of the Ta target, separating it from the moderator. The average proton beam current was set to 12 mA, corresponding to a pulsed beam operation with a duty cycle of 12%, and representing the maximum average current specified for radionuclide production in the accelerator Technical Design Report (TDR) of the HBS project [20]. Moderator thicknesses were varied from 1 to 20 cm with 1-cm increments. Reflector thicknesses were varied from 5 to 20 cm in 5-cm increments. Four natural Mo plates were placed inside the moderator: two large plates (12×24 cm^2; ~3 kg each; Plates A and D) and two smaller plates (12×12 cm^2; ~1.5 kg each; Plates B and C), all with a thickness of 1 cm. Plates C, B, and D, referred to as the lateral plates, were oriented facing the proton beam, with the 12 cm dimension extending along the beam axis.

Plate A, referred to as the axial plate, was placed on-axis and oriented facing the proton beam, with a 5-cm moderator layer upstream. The plate positions relative to the moderator were systematically varied. Initially, all plates were placed directly against the Al casing on the moderator side. The plates were then displaced in 0.5-cm increments up to 5 cm away from the casing. For the case of a 1-cm moderator, plates B, C, and D were located directly adjacent to the casing, while only Plate A was shifted along the beam axis due to spatial constraints.

4 Results and discussion

The configuration of Pb reflector and H_2O moderator, as specified in the TDR, was used as a reference to evaluate the effects of alternative moderators, reflectors, and geometric variations. The neutron energy spectra in the Mo plates (Fig. 2) show that the axial plate consistently receives the highest neutron flux across all energies and is therefore expected to yield the highest activity.

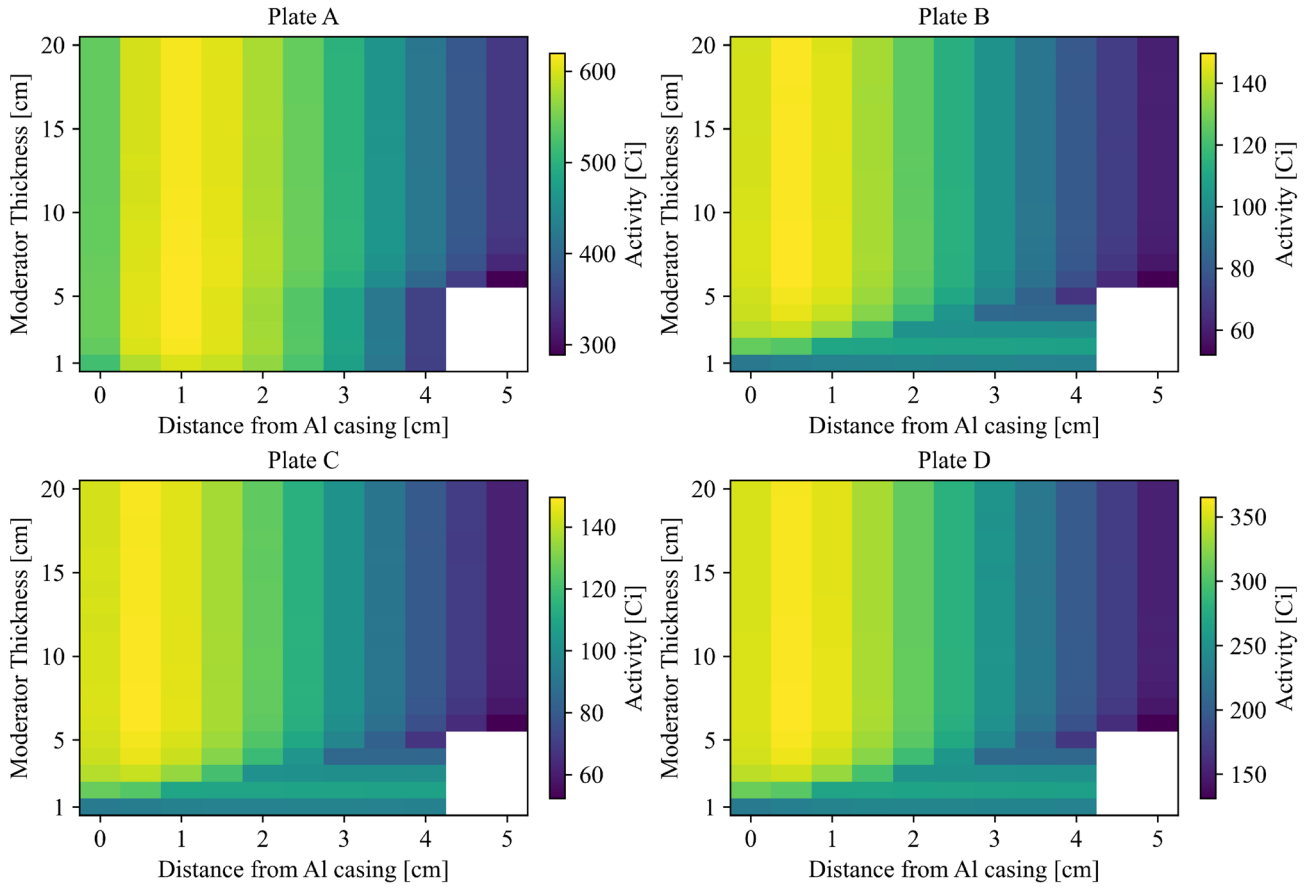

Fig. 4 ^{99}Mo activity (Ci) for a ZrH_2 moderator and Pb reflector (5 cm thickness)

Figures 3, 4, 5, 6 show the achievable ^{99}Mo activity after 6-day irradiation, corresponding to a total delivered proton charge of 1728 mA h (~6221 C) based on an average beam current of 12 mA.

The axial plate produces the highest ^{99}Mo activity, while the lateral plates yield significantly lower values. Plate-target distance is therefore the dominant factor for activation in the current TMR geometry, whereas increases in the moderator thickness have only a minor effect once a minimum thickness is reached.

Comparison of moderators (Figs. 3, 4, 5 and 6) highlights two distinct regimes. Hydrogen-based moderators (H_2O, ZrH_2) thermalize neutrons rapidly, so maximum activity is achieved with very thin moderator layers where the epithermal flux still dominates.

In contrast, moderators with lower slowing-down power (D_2O and Be) require substantially larger thicknesses to reach higher activity levels, with performance depending more strongly on moderator volume than on plate distance. These trends reflect the expected spectrum-shaping behavior: hydrogen-based moderators favor compact assemblies, whereas D_2O and Be require large moderator volumes to build up epithermal flux.

Figure 7 shows the total activity from all the plates for an irradiation time of 6 days for the highest yielding configuration (i.e. distance from Al casing and moderator thickness) for various reflectors, different reflector thicknesses, and corresponding moderator materials. As seen in Fig. 7, increasing reflector thickness generally enhances the total activity by reducing neutron leakage, though, for most cases, additional gains diminish beyond 10 cm reflector thickness.

A distinct behavior is observed for the Be-D_2O reflector–moderator combination, where the total activity continues to increase beyond 10 cm reflector thickness. This trend indicates a favorable coupling between efficient neutron reflection in Be and moderation in D_2O. As the Be reflector thickness increases, a larger fraction of neutrons is reflected to the moderator with minimal absorption losses, and D_2O enables further moderation while preserving flux. This results in a more pronounced increase in neutron flux contributing to the ^{98}Mo$(n,\gamma)^{99}$Mo reaction compared to Pb and MgO reflector cases. However, the apparent increase of the Be-D_2O configuration above the Be–Be case is influenced by the fixed, non-optimized plate position used in this study. As the moderator and reflector thicknesses increase, the spatial distribution of the neutron flux evolves and the location of the flux maximum shifts. Under these conditions, the fixed plate position becomes more favorable for the Be-D_2O configuration at larger reflector thicknesses. Additional tests with independently optimized plate positions show that Be–Be configuration yields the highest activity, while the Be-D_2O case remains close but does not exceed it.

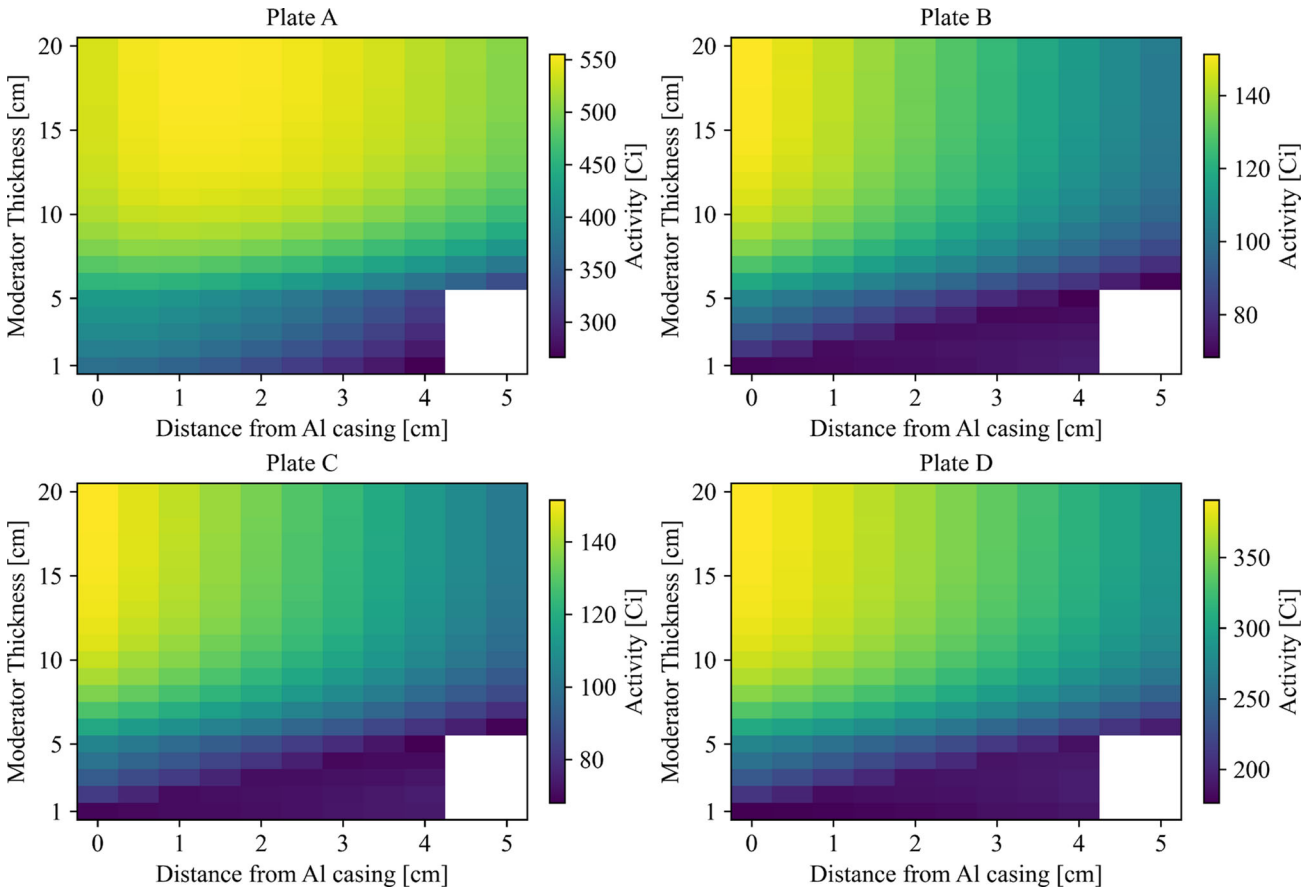

Fig. 5 ^{99}Mo activity (Ci) for a D_2O moderator and Pb reflector (5 cm thickness)

A Be moderator combined with a Be reflector yields the highest activities due to its favorable neutronic properties. However, neutron irradiation of Be is associated with swelling and tritium production, which can lead to material degradation and additional safety and waste-management challenges. In the present TMR design context, these drawbacks are likely to outweigh the performance gain and therefore limit the practical applicability of Be. Pb and MgO provide comparable neutronic performance, while MgO is preferred from an engineering standpoint due to its lower density, which enables larger reflector volumes without imposing excessive structural constraints.

Among moderators, ZrH_2 generally outperforms H_2O and D_2O across reflector configurations, except in combination with Be. However, the application of ZrH_2 requires a solid moderator design with active cooling, adding engineering complexity that may offset its performance advantage. D_2O provides higher activity than H_2O but is limited by cost, availability, and tritium production. Considering these trade-offs, the combination of an MgO reflector with an H_2O moderator emerges as the most practical configuration for reliable ^{99}Mo production.

Having established the MgO-H_2O system as the reference, with a moderator thickness of 5 cm and a reflector thickness of 20 cm, we investigated the effects of varying the thickness of Plate A on the total ^{99}Mo activity. This evaluation provides an estimate of the production potential under different Mo loading scenarios.

In Fig. 8, the activity for a 6-day irradiation is given as a function of the axial plate thickness. As shown in Fig. 8a, increasing axial plate thickness increases total activity. The activity maximum near 3 cm is caused by the competition between increasing target mass and the reduction of neutron flux with depth. While thicker targets contain more ^{98}Mo atoms, neutron attenuation limits the contribution of inner regions, so the increase in activity gradually saturates. In addition, resonance self-shielding may further suppress activation in thicker samples. Because the present method used for activity calculation is based on grouped neutron spectra, it does not fully resolve the fine resonance structure of the ^{98}Mo$(n,\gamma)^{99}$Mo reaction and may therefore underestimate self-shielding effects. The predicted activity for thicker targets should therefore be interpreted with some caution. This trade-off between total activity and specific activity is critical for generator applications because conventional alumina-column generators are originally developed for high specific activity (HSA) ^{99}Mo, for which high loading densities enable compact columns and high eluate concentrations. In contrast, neutron capture ^{99}Mo is intrinsically LSA, so generator concepts must compensate by using modified sorbents or column designs optimized for LSA ^{99}Mo [30–32]. Therefore, a 3-cm axial plate provides the best compromise between maximizing total activity and maintaining the specific activity for LSA generator compatibility.

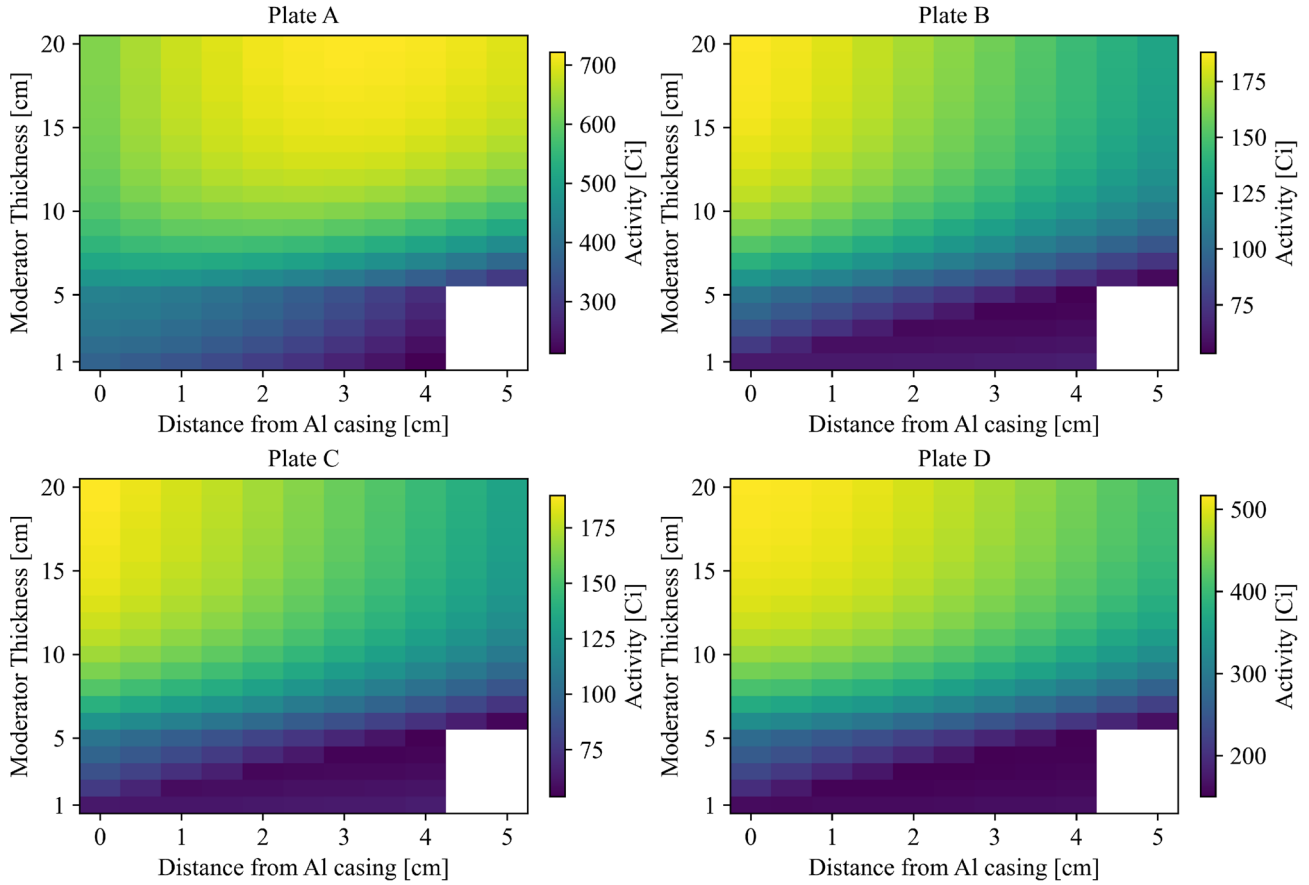

Fig. 6 ^{99}Mo activity (Ci) for a Be moderator and Pb reflector (5 cm thickness)

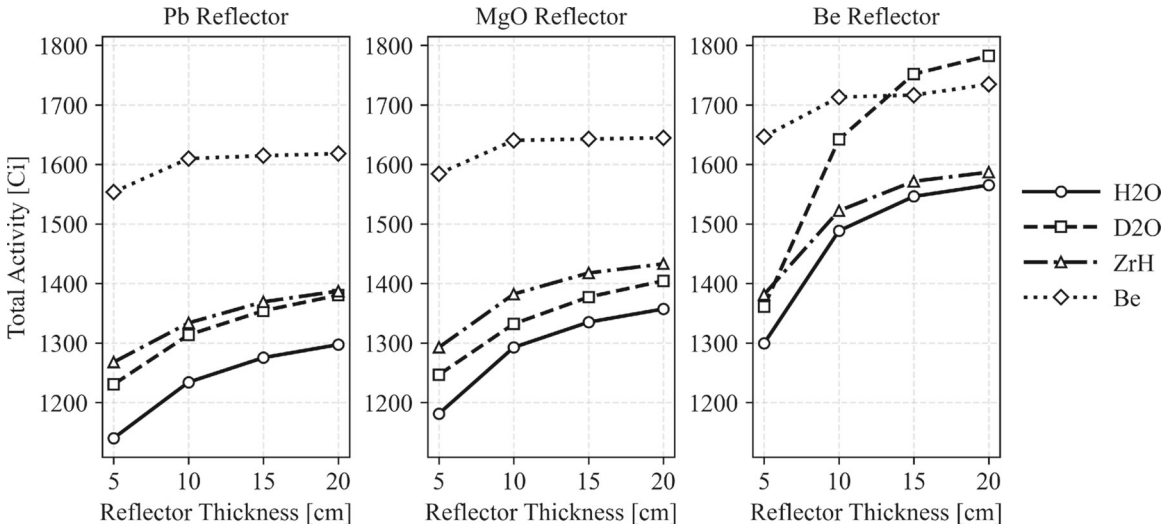

Fig. 7 Total ^{99}Mo activity (sum of axial and lateral plates) for different reflector thicknesses and various reflector materials with several moderator materials

Figure 8b further shows that the activity comparable to the four-plate setup can be achieved using a single axial plate, though this would require thicknesses exceeding 4 cm. At such dimensions uncertainties in neutron self-shielding become significant and require dedicated experimental validation [33].

Under the optimized MgO-H_2O configuration with a 3-cm-thick axial plate and 6-day irradiation, production could reach ~2,400 Ci, sufficient to meet Germany's current weekly demand. The corresponding specific activity levels are compatible with LSA generator concepts. Future work should focus on quantifying self-shielding effects, refining generator design, developing automated plate handling, addressing radiation safety, and assessing long-term operational performance.

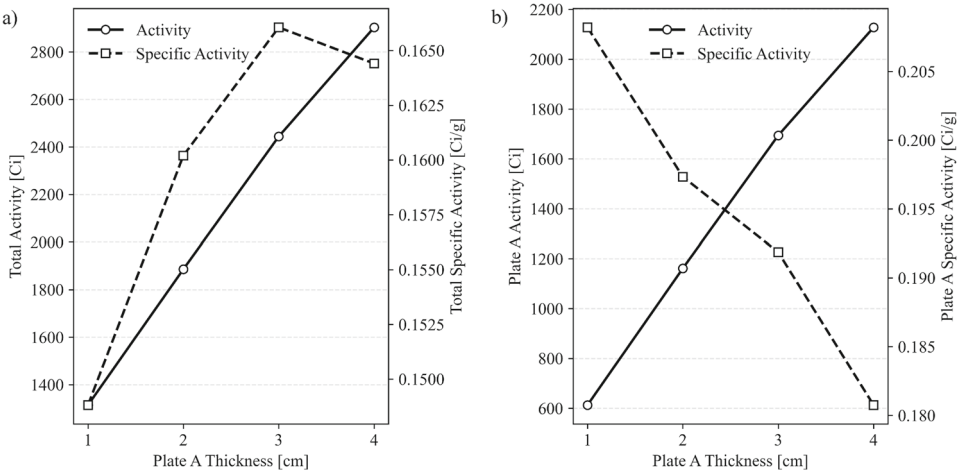

Fig. 8 ^{99}Mo activity and specific activity for the MgO-H_2O system as a function of axial plate thickness **a** axial plus lateral plates combined, **b** axial plate only

5 Conclusions

This study investigated the feasibility of producing ^{99}Mo via the ^{98}Mo$(n,\gamma)^{99}$Mo route in an accelerator-driven neutron source modeled after the HBS design. The simulations were performed for a 70 MeV, 12 mA proton beam impinging on a Ta target capable of sustaining heat loads up to 3 kW/cm^2 under active cooling. Various moderator configurations (H_2O, D_2O, ZrH_2, Be) and reflector materials (Pb, MgO, Be) were systematically evaluated.

The results of the simulations show that:

- Mo plate–Ta target proximity is the dominant factor for activation, while moderator thickness has only a secondary effect once a minimum value is reached.
- Hydrogen-based moderators (H_2O, ZrH_2) favor compact assemblies, whereas D_2O and Be require thicker moderator volumes to reach higher activities.
- An MgO reflector combined with an H_2O moderator is the most practical configuration, balancing performance with engineering feasibility and regulatory acceptance.
- In the four-plate layout, a 3 cm thickness for the axial plate (and 1 cm for the lateral plates) provides the best compromise between total activity and specific activity, ensuring generator compatibility under LSA conditions.
- Irradiation at the axial position is significantly more efficient than lateral positions; thus, a single thicker axial plate could in principle achieve the ~ 2,400 Ci needed to cover Germany's weekly demand. However, neutron self-shielding in thick plates remains a critical uncertainty that requires experimental validation.

Overall, the study demonstrates that accelerator-based neutron sources such as the one proposed by the HBS could offer a viable non-^{235}U-fission route to ^{99}Mo production. Future work should focus on experimental quantification of self-shielding in thicker plates, optimization of a single-plate design, generator development tailored to LSA ^{99}Mo, automation of plate handling, and assessment of long-term radiation safety and operational performance.

Funding Open Access funding enabled and organized by Projekt DEAL. This research has been financially supported by the German Federal Ministry of Research, Technology, and Space (BMFTR) in the project 99MoBEST, funding number 02NUK080B.

Data availability The data that support the findings in this study are available from the corresponding author upon reasonable request. The manuscript has associated data in a data repository.

Declarations

Conflict of interest The authors have no conflict of interest to declare that are relevant to the content of this article.

References

1. NEA, *The Supply of Medical Radioisotopes: 2019 Medical Isotope Demand and Capacity Projection for the 2019–2024 Period* (OECD Publishing, Paris, 2019)
2. Deutscher Bundestag, Drucksache 17/3142, 2010
3. ASNC, Alert: Significant Mo-99 shortage expected in coming weeks, https://www.asnc.org/news/alert-significa-nt-mo-99-shortage-expected-in-coming-weeks/Accessed 26 Aug 2025
4. J. Jaroszewicz, Z. Marcinkowska, K. Pytel, Production of fission product ^{99}Mo using high-enriched uranium plates in polish nuclear research reactor MARIA: technology and neutronic analysis. Nukleonika **59**(2), 43–52 (2014)
5. S.K. Lee, S. Lee, M. Kang, K. Woo, S. Woo Yang, J. Lee, Development of fission ^{99}Mo production process using HANARO. Nucl. Eng. Technol. **52**, 1517–1523 (2020)
6. J.J. Toth, L.R. Greenwood, C.Z. Soderquist, R.S. Wittman, B.D. Pierson, K.A. Burns, C.A. Lavender, C.L. Painter, E.F. Love, D.E. Wall, Production of Molybdenum-99 using neutron capture methods. PNNL-19895, RPT-59331–01 Rev 0, Pacific Northwest National Laboratory (2011)
7. M. Blaauw, D. Ridikas, S. Baytelesov, P.S. Bedregal Salas, Y. Chakrova, C. Eun-Ha, R. Dahalan, A.H. Fortunato, R. Jacimovic, A. Kling, L. Munoz, N.M.A. Mohamed, D. Párkányi, T. Singh, V.D. Duong, Estimation of 99Mo production rates from natural molybdenum in research reactors. J. Radioanal. Nucl. Chem. **311**, 409–418 (2017)
8. R. Seviour, H. Owen, Bailey compact accelerator based neutron source for Technetium-99m production. Proceedings of IPAC2016 Busan Korea ISBN 978–3–95540–147–2:1946–1949 (2016)
9. M. Ohta, S. Kwon, S. Sato, K. Ochiai, H. Suzuki, Investigation of the Mo-99 radioisotope production by d-Li neutron source. Nucl. Eng. Technol. **15**, 261–266 (2018)
10. Non-HEU production technologies for Molybdenum-99 and technetium-99m. IAEA nuclear energy series, ISSN 1995–7807; no. NF-T-5.4. Vienna: International Atomic Energy Agency, (2013)
11. Ann Fong, Timothy I. Meyer, Krista Zala (Eds.), Making medical isotopes: report of the task force on alternatives for medical-isotope production, TRUMF, Vancouver, 2008 https://www.triumf.ca/report-medical-isotope-production
12. OECD NEA Data Bank, JANIS Book of neutron-induced cross-sections (2020) https://www.oecd-nea.org/janis/book/book-neutron-2020-09.pdf
13. Y. Nagai, Y. Hatsukawa, Production of 99Mo for Nuclear Medicine by 100Mo(n,2n)99Mo. J. Phys. Soc. Jpn. **3**(3), 033201 (2009)
14. L. Fu, R. Liu, Optimization of photon neutron reaction for medical isotope Molybdenum-99 production. Int. J. Pharm Biol Sci **4**(2), 90–96 (2015)
15. T. Michael Martin, T. Harahsheh, B. Munoz, Z. Hamoui, R. Clanton, J. Douglas, P. Brown, G. Akabani, Production of ^{99}Mo/^{99m}Tc via photoneutron reaction using natural molybdenum and enriched ^{100}Mo: part 1, theoretical analysis. J. Radioanal. Nucl. Chem. **314**, 1051–1062 (2017)
16. A. Shaikh, T.S. Dixit, A.P. Deshpande, R. Krishnan, Comparative Simulation Study of Direct and Indirect Target Production of ^{99}Mo with Linear Accelerator SAMEER. J. Adv. Radiol. Med. Imag. **4**(1), 1–7 (2019)
17. W.T. Diamond, A radioactive ion beam facility using photofission. Nucl. Instrum. Methods **432**, 471–482 (1999)
18. National Academies of Sciences, Engineering, and Medicine, Molybdenum-99 for Medical Imaging. National Academies Press, Washington, DC (2016). Available at: https://www.ncbi.nlm.nih.gov/books/NBK396170/
19. P. Martini, A. Boschi, G. Cicoria, F. Zagni, A. Corazza, L. Uccelli, M. Pasquali, G. Pupillo, M. Marengo, M. Loriggiola et al., In-house cyclotron production of high-purity Tc-99m and Tc-99m radio pharmaceuticals. Appl. Radiat. Isotopes **139**, 325–331 (2018). https://doi.org/10.1016/j.apradiso.2018.05.033
20. T. Brückel, T. Gutberlet (Eds.) Opportunities for research with neutrons at the 254 next generation facility HBS: overview of the high brilliance neutron source (HBS) technical design report, Vol. 9. Schriften des Forschungszentrums Jülich Allgemeines/General. Forschungszentrum Jülich, Jülich (2023)
21. D. Shabani, S.T. Rangaiah, C. Langer et al., Benchmarking of the PHITS simulation code using neutron activation experiments for reliable calculations of neutron fields. J. Radioanal. Nucl. Chem. **334**, 2981–2989 (2025). https://doi.org/10.1007/s10967-025-10020-6
22. D.A. Brown et al., ENDF/B-VIII.0: the 8th major release of the nuclear reaction data library with CIELO-project cross sections, new standards and thermal scattering data. Nucl. Data Sheets **148**, 1–142 (2018)
23. T. Sato, Y. Iwamoto, S. Hashimoto, T. Ogawa, T. Furuta, S. Abe, T. Kai, Y. Matsuya, N. Matsuda, Y. Hirata, T. Sekikawa, L. Yao, P.E. Tsai, H.N. Hunter, H. Iwase, Y. Sakaki, K. Sugihara, N. Shigyo, L. Sihver, K. Niita, Recent improvements of the particle and heavy ion transport code system—PHITS version 3.22. J. Nucl. Sci. Technol. **61**, 127–135 (2024). https://doi.org/10.1080/00223131.2023.2275736
24. K. Shibata, O. Iwamoto, T. Nakagawa, N. Iwamoto, A. Ichihara, S. Kunieda, S. Chiba, K. Furutaka, N. Otuka, T. Ohsawa, T. Murata, H. Matsunobu, A. Zukeran, S. Kamada, JENDL-4.0: a new library for nuclear science and engineering. J. Nucl. Sci. Technol. **48**(1), 1–30 (2011). https://doi.org/10.1080/18811248.2011.9711675
25. N.S. Schmidt, D. Shabani, J. Li et al., Development of an epithermal and fast neutron target station for the high brilliance neutron source. Eur Phys J Plus **140**, 171 (2025). https://doi.org/10.1140/epjp/s13360-025-06100-x
26. B.P. Sharma, Nuclear reactors: moderator and reflector materials, in *Encyclopedia of Materials: Science and Technology*. (Elsevier, Oxford, 2001), pp.6365–6369. https://doi.org/10.1016/B0-08-043152-6/01232-3
27. Pacific Northwest National Laboratory (PNNL) *Data Mining Analysis and Modeling Cell Compendium of Material Composition Data for Radiation Transport Modeling*. PNNL-15870, Rev. 2; 200-DMAMC-128170, Apr 2021. (2021)
28. J. Baggemann, T. Gutberlet, P. Zakalek, J. Wolters, U. Rücker, E. Mauerhofer, J. Li, Q. Ding, T. Loewenhoff, D. Dorow-Gerspach, Y. Bessler, T. Brückel, High power target for the high brilliance neutron source. Nucl Instrum Methods Phys Res A **1069**, 169930 (2024). https://doi.org/10.1016/j.nima.2024.169930
29. P. Mastinu, J. Praena, G. Martín-Hernández, N. Dzyiuk, G. Prete, R. Capote, M. Pignatari, A. Ventura, Status of the LEgnaro NeutrOn source facility (LENOS). Phys. Procedia **26**, 261–273 (2012)
30. R. Chakravarty, R. Ram, A. Dash, M.R.A. Pillai, Preparation of clinical-scale 99Mo/99mTc column generator using neutron activated low specific activity 99Mo and nanocrystalline γ-Al2O3 as column matrix. J. Radioanal. Nucl. Chem. **293**, 479–484 (2012). https://doi.org/10.1007/s10967-012-1741-0
31. J. Wang, R. Gao, Q. Huang, X. Yin, M. Lin, S. Cao, D. Chen, F. Fan, X. Wu, Z. Qin, Z. Guo, J. Bai, J. Chu, W. Tian, C. Tan, B. Li, N. Cheng, Z. Jia, Practicality of hierarchically macro/mesoporous γ-Al_2O_3 as a promising sorbent in the preparation of low specific activity ^{99}Mo/^{99m}Tc generator. Appl. Radiat. Isot. **178**, 109986 (2021). https://doi.org/10.1016/j.apradiso.2021.109986

32. M. Michel, F. Sudbrock, B. Neumaier et al., Comparison of standard and modified ^{99}Mo/^{99m}Tc radionuclide generators. J. Radioanal. Nucl. Chem. **334**, 7255–7263 (2025). https://doi.org/10.1007/s10967-025-10423-5
33. D. Akkaya, The calculation of self-shielding correction factors for large samples in ^{241}Am–Be isotopic neutron source. Appl. Radiat. Isot. **179**, 109990 (2022). https://doi.org/10.1016/j.apradiso.2021.109990